Journal of Alloys and Compounds 480 (2009) 777–781

Contents lists available at ScienceDirect

Journal of Alloys and Compounds

journal homepage: www.elsevier.com/locate/jallcom

Effect of Ba-site substitution by Sr on ultrasonic velocity and electron–phonon coupling constant of $DyBa_{2-x}Sr_xCu_3O_{7-\delta}$ superconductors

N.A. Rasih, A.K. Yahya*

School of Physics and Materials Studies, Universiti Teknologi Mara, 40450 Shah Alam, Selangor, Malaysia

ARTICLE INFO

Article history:
Received 27 August 2008
Received in revised form 11 February 2009
Accepted 14 February 2009
Available online 27 February 2009

Keywords:
High-T_c superconductor
Ultrasonics
Elasticity
Electron–phonon interaction

ABSTRACT

Ultrasonic longitudinal velocity measurements between 80 K and 280 K and shear velocity measurements between 80 K and 230 K have been performed in polycrystalline superconducting $DyBa_{2-x}Sr_xCu_3O_{7-\delta}$ ($x = 0$, 0.3, 0.6) samples utilizing the pulsed-echo-overlap technique. Substitution of Sr caused the percentage change in shear velocity to gradually decrease with x from 1.3% ($x = 0$) to 0.8% ($x = 0.6$). Longitudinal velocity showed initial increase from 1.7% ($x = 0$) to 1.9% ($x = 0.3$) before decreasing to 1.1% ($x = 0.6$). A step-like longitudinal anomaly was observed at 240 K for $x = 0$ and $x = 0.3$ and at 260 K for $x = 0.6$. Sr substitution however, reduced the slope change of the step-like anomaly from 0.0078% K^{-1} ($x = 0$) to 0.0043% K^{-1} ($x = 0.3$) and 0.0023% K^{-1} ($x = 0.6$). A comparison between experimental data and calculated lattice anharmonicity curve based on the model by Lakkad [S.C. Lakkad, J. Appl. Phys. 42 (1971) 4277–4281] showed that the large deviation of the experimental velocity curves for $x = 0$, 0.3 from the calculated curves is strongly influenced by existence of the step-like longitudinal anomalies. The longitudinal step-like anomalies are suggested to be due to oxygen ordering taking place in Cu–O chains during a phase transition. The reduction in the slope change of the step-like anomalies indicates some degree of weakening of oxygen ordering due to the Sr substitution. Sr substitution also has the effect of lowering the calculated electron–phonon coupling constant (λ).

1. Introduction

The discovery of superconductivity in La-based [1], Y-based [2], Tl-based [3], Bi-based [4], and other cuprates [5] has led to intense research efforts directed towards understanding the underlying mechanism of high-temperature superconductivity. However, until today the definite mechanisms that control high-temperature superconductivity remain an open question. Interestingly, the possibility of lattice contribution to the electron pairing mechanism has been supported by a number of experimental evidences [6,7]. The ultrasonic method, which is sensitive to lattice instabilities and phase transitions, was found to be very useful to probe bulk property changes of ceramic materials such as glasses [8–11], magnetoresistance materials [12–15], and also high-temperature superconductors [16–24 and references therein]. In the latter, step-like velocity anomalies above 200 K indicating sudden or unexpected elastic hardening taking place in superconducting samples have been observed in several RE123 [16,17], RE1113 [20] and Bi-based samples [18,21]. The step-like anomalies were found to be oxygen related but its relationship to superconductivity is still not clear [23].

On the other hand, quite extensive investigations involving elemental substitutions in high-temperature superconductors have been performed with the aim of improving superconducting properties and also to investigate the role played by different atomic sites in a superconducting material. In the case of RE123, Sr substitutions at the Ba site were reported to cause a non-linear drop in critical temperature, T_c [25,26]. The slow decrease in T_c was suggested to be related to changes in copper–oxygen bond length [25] or changes in planar weight distribution due to substitution of lighter Sr^{2+} in place of heavier Ba^{2+} [27]. Ultrasonic velocity studies on $REBaCu_3O_{7-\delta}$ were also able to identify accompanying bulk changes as a result of elemental substitutions [17,28] but the number of such studies is limited.

In addition, ultrasonic velocity data can also be used to compute the acoustic Debye temperature, θ_D and the electron–phonon coupling constant, λ. In the BCS theory, for the weak coupling limit, λ is related to T_c by the formula [29],

$$T_c = 1.13\theta_D e^{-1/\lambda} \quad (1)$$

Elemental substitution in (Er,Pr)123 [29], (Dy,Pr)1113 [29] and Zn-substituted Gd1113 [30], was reported to cause a lowering of λ. As such, it is interesting to investigate the effect of elemental substitution at the Ba-site not only on elastic properties of $DyBa_2Cu_3O_{7-\delta}$ but also on its electron–phonon coupling constant (λ).

* Corresponding author. Tel.: +60 355444561; fax: +60 355444562.
E-mail address: ahmad191@salam.uitm.edu.my (A.K. Yahya).

0925-8388/$ – see front matter © 2009 Elsevier B.V. All rights reserved.
doi:10.1016/j.jallcom.2009.02.055

Table 1
$T_{c\ zero}$, $T_{c\ onset}$, room-temperature resistivity, lattice parameters and unit cell volume, V, for $DyBa_{2-x}Sr_xCu_3O_{7-\delta}$ ($x = 0$, 0.3, 0.6).

Sr content (x)	$T_{c\ zero}$ (K) ±0.1	$T_{c\ onset}$ (K) ±0.1	Resistivity at 300 K (mΩ cm)	Lattice parameters			Unit Cell Volume V (Å^3)
				a	b	c	
0	88.1	95.7	5.83 ± 0.02	3.837 ± 0.004	3.908 ± 0.003	11.708 ± 0.003	175.6 ± 0.2
0.3	77.7	85.1	7.34 ± 0.02	3.832 ± 0.003	3.878 ± 0.003	11.672 ± 0.003	173.5 ± 0.2
0.6	61.1	78.1	4.25 ± 0.02	3.817 ± 0.006	3.877 ± 0.006	11.630 ± 0.005	172.1 ± 0.2

This paper reports on longitudinal (80–280 K) and shear (80–230 K) velocity measurements in superconducting $DyBa_{2-x}Sr_xCu_3O_{7-\delta}$ ($x = 0$, 0.3, 0.6) polycrystalline samples. The lattice anharmonicity model as discussed by Lakkad [31] was used as a comparison to evaluate the extent of deviation of the elastic behavior at high temperatures. The effect of Sr-substitution on elastic property, elastic anomaly and λ of the samples was analyzed. Results of electrical resistance (d.c.) measurement, X-ray diffraction analyses and microstructure investigations using scanning electron microscope (SEM) are also presented.

2. Experimental details

The $DyBa_{2-x}Sr_xCu_3O_{7-\delta}$ ($x = 0$–0.6) samples were prepared from high purity (>99.99%) chemicals using conventional solid-state synthesis by mixing appropriate amounts of Dy_2O_3, $BaCO_3$, $SrCO_3$ and CuO powders. The materials were ground in an agate mortar then calcined in air at around 900 °C for 48 h with several intermittent grindings and oven cooled. The powders were then reground before they were pressed into pellets of 13 mm diameter and 2–3 mm thickness under a load of 6–7 tons. The pellets were then sintered at 910 °C for 24 h and slow cooled to room temperature at the rate of 24 °C h^{-1}. Based on comparisons of lattice parameters and critical temperature, T_c of Dy123 in this work to previous reports on RE123 samples [32–34], the oxygen deficiency, δ was estimated to be 0.1. The substituted samples were suggested to have the same oxygen contents ($\delta \sim 0.1$) as previous reports on Sr-substituted RE123 showed very small variations in oxygen content [25,35].

Electrical resistance (d.c.) measurements of the samples were carried out using the standard four-point-probe technique with silver paste contacts in a Janis cryostat model CCS-350ST and controlled by a LakeShore model 330 temperature controller. Temperature measurements were made using GaAlAs diode sensor. Powder X-ray diffraction (XRD) analyses using Rigaku model D/MAX 2000 PC with Cu K_α radiation source was used to confirm the phase structure of the samples. The microstructure was observed by JEOL model JSM-6360LA scanning electron microscope.

Sound velocity measurements were carried out using a Matec 7700 system which utilizes the pulse-echo-overlap technique. A quartz transducer was bonded on the polished samples surface using Nonaq stopcock grease. Sound velocity was propagated along the direction of pressing using an x-cut (longitudinal) and a y-cut (shear) transducer with a carrier frequency of 9 MHz. These measurements were performed in a Janis model VNF100T liquid nitrogen cryostat and the temperature was changed at a rate of 1 K min^{-1} during warming and cooling. The pulse-echo-overlap system used was capable of measuring changes to 1 part in 10^7 in ultrasonic transit time, for relative velocity measurements.

As a comparison to the measured temperature dependent sound velocity curves, one of several anharmonicity models [31,36,37] can be plotted together with the velocity curves to illustrate the extent of deviation of the velocity behavior from the calculated curve at high temperatures [16,38]. The simple model proposed by Lakkad [31] which uses a phenomenological model of anharmonic oscillator together with the Debye lattice vibration spectrum was chosen in this work. It has been shown that, the model is in a better position to predict elastic behavior and lattice contribution to elastic moduli especially for temperatures below 150 K [39]. The equation proposed by Lakkad [31] to predict the temperature variation of the elastic constant $E(T)$ of a material is given in Eq. (2) below;

$$E(T) = E_o \left[1 - kF\left(\frac{T}{\theta_D}\right)\right] \tag{2}$$

where E_o is the elastic constant at 0 K, k is a constant and θ_D is the Debye temperature. $F(T/\theta_D)$ in Eq. (2) is given in Eq. (3) below.

$$F\left(\frac{T}{\theta_D}\right) = 3\left(\frac{T}{\theta_D}\right)^4 \int_0^{\theta_D/T} \frac{x^3 e^x}{(e^x - 1)} dx \tag{3}$$

Here, $x = hf/k_BT$ where h is the Planck constant, f is the frequency of vibration and k_B is the Boltzmann constant. The temperature dependence of the sound velocity curves was fitted to this model using elastic constants at two different temperatures along the curve together with the computed Debye temperature (θ_D).

3. Results and discussion

The XRD patterns (Fig. 1) showed all samples consist of single phased 123 orthorhombic structures with space group Pmmm. Table 1 showed values of $T_{c\ zero}$, $T_{c\ onset}$, room-temperature resistivity, lattice parameters and unit cell volume for all samples. Sr substitution caused reduction in lattice parameters a, b, and c and unit cell volume, V. Temperature dependent electrical resistivity measurements (Fig. 2) using the standard four-point-probe method showed metallic normal state behavior for all samples. The Sr substitution also showed a non-linear drop of $T_{c\ zero}$ with a slightly larger drop of 16.6 K from $x = 0.3$ to $x = 0.6$ compared to a drop of 10.4 K from $x = 0$ to $x = 0.3$.

SEM micrographs of the internal section of the samples (Fig. 3) showed irregular shaped grains in addition to the existence of voids and pores. The estimated average grain size for superconducting $DyBa_2Cu_3O_{7-\delta}$ was between 10 μm and 12 μm (Fig. 3(a)). The microstructures of $DyBa_{1.7}Sr_{0.3}Cu_3O_{7-\delta}$ (Fig. 3(b)) and $DyBa_{1.4}Sr_{0.6}Cu_3O_{7-\delta}$ (Fig. 3(c)) are generally similar with aver-

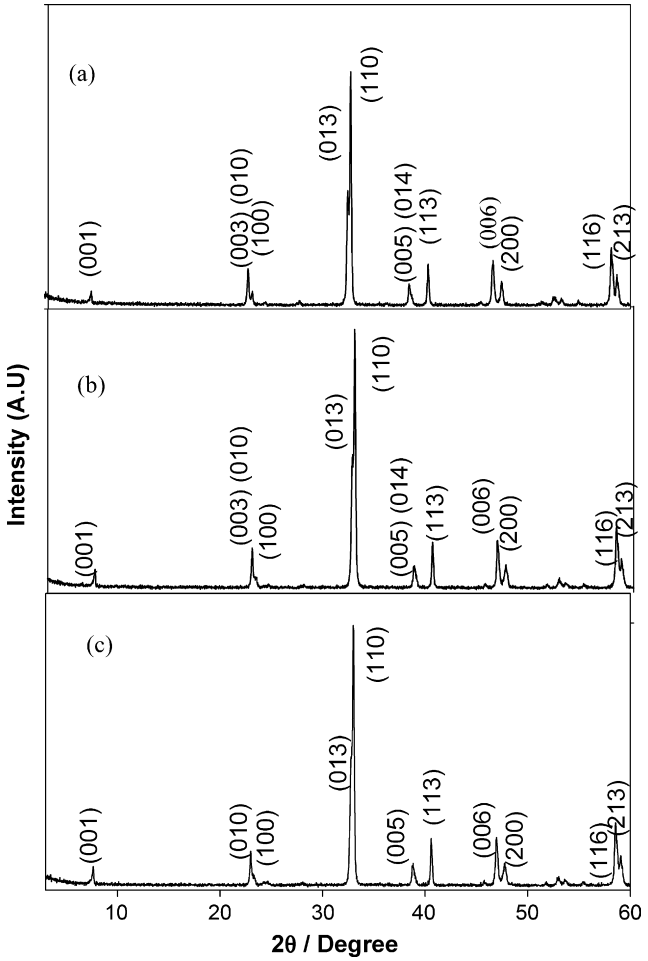

Fig. 1. X-ray powder diffractogram of superconducting $DyBa_{2-x}Sr_xCu_3O_{7-\delta}$ (a) $x = 0$; (b) $x = 0.3$; and (c) $x = 0.6$.

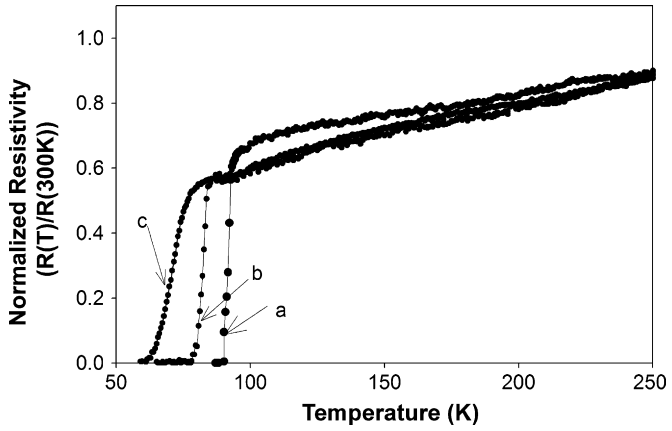

Fig. 2. Resistance versus temperature curve of $DyBa_{2-x}Sr_xCu_3O_{7-\delta}$ (a) $x=0$; (b) $x=0.3$; and (c) $x=0.6$.

age grains sizes between 4 μm and 6 μm. The correction for porosity was achieved by comparing the measured sample density to the non-porous sample density derived from X-ray diffraction data [16]. The ideal sound velocity was calculated from the measured velocity using the relation suggested in Ref. [40];

$$v_i = v\sqrt{\frac{\rho_i}{\rho}} \tag{4}$$

where v_i is the non-porous sample velocity, ρ_i is the ideal density calculated from X-ray data and v is the measured velocity.

As the ultrasonic wavelength used in this study was much larger than the average grain size, the polycrystalline ceramic samples can be approximated by an isotropic-elastic medium to calculate the longitudinal and shear elastic moduli [38,40]. In this approximation, the longitudinal and shear moduli are given by $C_L(=\rho v_l^2)$ and $\mu(=\rho v_s^2)$, respectively where ρ is the density, v_l is the longitudinal velocity and v_s is the shear velocity [40]. The related elastic stiffness moduli, bulk modulus (B) and Young's modulus (Y) were determined using the measured ultrasonic wave velocity values. The acoustic Debye temperature (θ_D) was calculated using the standard formula given in Ref. [41] below;

$$\theta_D = \frac{h}{k_B}\left(\frac{3N}{4\pi V}\right)^{1/3} v_m \tag{5}$$

where h is the Planck constant, k_B is the Boltzman constant, N is the number of independent three-dimensional Einstein oscillators, V is the unit cell volume calculated from lattice parameter values and v_m is the mean velocity. The mean velocity is given by:

$$\frac{3}{v_m^3} = \frac{1}{v_l^3} + \frac{2}{v_s^3} \tag{6}$$

The sample porosity, density (ρ), absolute longitudinal (v_l) and shear velocities (v_s) at 80 K, longitudinal modulus (C_L), shear modulus (μ), bulk modulus (B), Young's modulus (Y), Debye temperature θ_D and electron–phonon coupling constant (λ) are tabulated in Table 2. The values which were corrected for porosity using Eq. (4) is given in Table 3.

Substitution of Sr in $DyBa_{2-x}Sr_xCu_3O_{7-\delta}$ caused an increase in v_l, v_s, C_L, B, Y and θ_D (Table 3). The θ_D for superconducting $DyBa_2Cu_3O_{7-\delta}$ was 397 K and is comparable to acoustic Debye temperature values reported for other $REBa_2Cu_3O_{7-\delta}$ superconductors [16,17,28]. The increase in absolute longitudinal and shear velocities at 80 K with x may be related to the decrease of cell volume as a result of substitution of smaller Sr^{2+} (ionic radius: 1.25 Å) for Ba^{2+} (ionic radius: 1.42 Å). This volume change may have caused changes in interatomic length and bonding strength which were detected

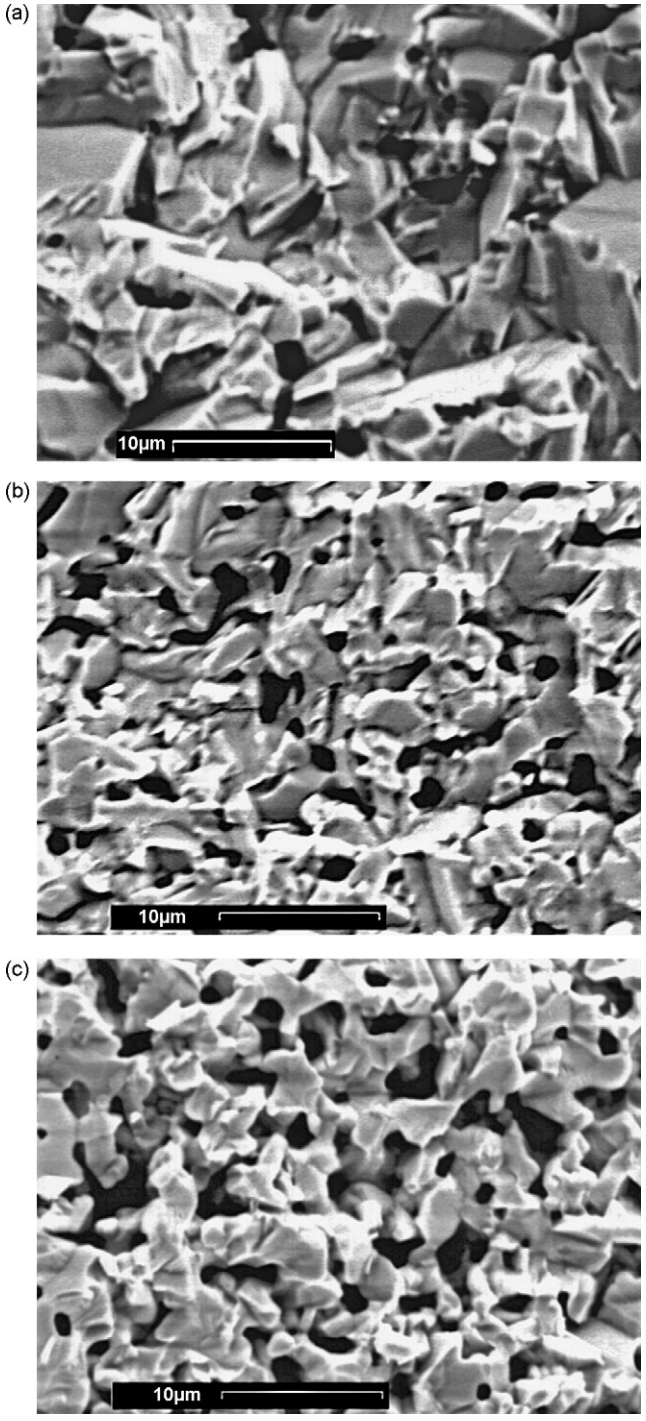

Fig. 3. Scanning electron micrograph (SEM) of internal section of $DyBa_{2-x}Sr_xCu_3O_{7-\delta}$ (a) $x=0$, (b) $x=0.3$ and (c) $x=0.6$.

by both longitudinal and shear phonons and are reflected by the increase in velocity for both modes with increasing Sr [21]. Interestingly, the substitution of Sr for Ba which caused a decrease in T_c has also caused an increase in θ_D (Table 3). Further calculation however showed that this was caused by the reduction in electron–phonon coupling constant, λ with increasing Sr. A similar reduction in λ was also reported for $(Er,Pr)Ba_2Cu_3O_{6.9}$ [29], $(Dy,Pr)BaSrCu_3O_{7-\delta}$ [29] and $GdBaSr(Cu,Zn)_3O_{7-\delta}$ [30].

Figs. 4 and 5 show the temperature dependencies of the longitudinal (80–280 K) and shear (80–230 K) relative velocity changes, respectively, for all samples together with the calculated lattice

Table 2
Sr-content (x), density, porosity, longitudinal velocity (v_l), shear velocity (v_s), longitudinal modulus (C_L), shear modulus (μ), bulk modulus (B), Young's modulus (Y), Debye temperature (θ_D) and electron–phonon coupling (λ_{BCS}) measured at 80 K for $DyBa_{2-x}Sr_xCu_3O_{7-\delta}$ $x = 0$, 0.3 and 0.6. The values were not corrected for porosity.

X	Density ($g\,cm^{-3}$)	Porosity (%)	v_l ($km\,s^{-1}$)	v_s ($km\,s^{-1}$)	C_L (GPa)	μ (GPa)	B (GPa)	Y (GPa)	θ_D (K)	λ_{BCS}
0	6.16 ± 0.03	11.7	4.61 ± 0.02	2.70 ± 0.01	131 ± 2	44.8 ± 0.5	71.0 ± 0.7	111 ± 4	372 ± 2	0.64 ± 0.01
0.3	6.16 ± 0.02	10.9	5.02 ± 0.02	2.72 ± 0.01	156 ± 1	45.5 ± 0.6	94.9 ± 0.7	118 ± 3	379 ± 2	0.59 ± 0.01
0.6	6.02 ± 0.03	11.9	5.10 ± 0.06	2.86 ± 0.04	156 ± 5	49.0 ± 1.4	91.1 ± 2.0	125 ± 3	398 ± 6	0.50 ± 0.01

Table 3
Sr-content (x), density, porosity, longitudinal velocity (v_l), shear velocity (v_s), longitudinal modulus (C_L), shear modulus (μ), bulk modulus (B), Young's modulus (Y), Debye temperature (θ_D) and electron–phonon coupling (λ_{BCS}) measured at 80 K for $DyBa_{2-x}Sr_xCu_3O_{7-\delta}$ $x = 0$, 0.3 and 0.6. The values were corrected for porosity.

X	Density ($g\,cm^{-3}$)	v_l ($km\,s^{-1}$)	$_{vs}$ ($km\,s^{-1}$)	C_L (GPa)	μ (GPa)	B (GPa)	Y (GPa)	θ_D (K)	λ_{BCS}
0	6.98 ± 0.03	4.90 ± 0.02	2.87 ± 0.01	167 ± 2	57.5 ± 0.5	91.1 ± 0.7	142 ± 4	397 ± 2	0.61 ± 0.01
0.3	6.92 ± 0.02	5.32 ± 0.02	2.88 ± 0.01	196 ± 1	57.4 ± 0.6	119.7 ± 0.7	148 ± 3	401 ± 2	0.57 ± 0.01
0.6	6.83 ± 0.03	5.43 ± 0.06	3.04 ± 0.04	202 ± 5	63.1 ± 1.4	117.3 ± 2.0	161 ± 3	425 ± 6	0.49 ± 0.02

anharmonicity curve calculated using the Lakkad model given in Ref. [31]. $DyBa_2Cu_3O_{7-\delta}$ showed a longitudinal velocity change of 1.7% which deviated from the calculated curve above 200 K (Fig. 4(a)). A step-like anomaly was observed around 240 K for $DyBa_2Cu_3O_{7-\delta}$ indicating pronounced lattice stiffening. Similarly for $DyBa_{1.7}Sr_{0.3}Cu_3O_{7-\delta}$ longitudinal velocity showed a change of 1.9% (Fig. 4(b)) and deviated from anharmonicity curve above 135 K. A step-like anomaly was also observed around 240 K for $DyBa_{1.7}Sr_{0.3}Cu_3O_{7-\delta}$. However, $DyBa_{1.4}Sr_{0.6}Cu_3O_{7-\delta}$ showed the smallest change in longitudinal velocity of 1.1% (Fig. 4(c)) and displayed good agreement with the calculated curve up to 260 K where a weak step-like anomaly was observed. The measured changed in slope of the step-like anomalies were 0.0078% K^{-1} ($x = 0$), 0.0043% K^{-1} ($x = 0.3$) and 0.0023% K^{-1} ($x = 0.6$). This showed that besides the observed temperature shift of the step-like anomaly for $x = 0.6$, the Sr substitutions also have the effect of gradually reducing the change in slope. For the shear mode, ultrasonic velocity for $DyBa_2Cu_3O_{7-\delta}$ and $DyBa_{1.7}Sr_{0.3}Cu_3O_{7-\delta}$ showed a velocity change of 1.3% and 1.1%, respectively, and both curves deviated from the anharmonicity curve above 140 K. $DyBa_{1.4}Sr_{0.6}Cu_3O_{7-\delta}$ showed the smallest percentage change in shear velocity of 0.8% and the velocity curve showed good agreement with the calculated curve between 80 K and 220 K.

The variation of velocity change for both longitudinal and shear modes indicates strong influence of Sr substitution on elastic properties. The strong deviation of velocity curves from the respective anharmonicity curves for $DyBa_2Cu_3O_{7-\delta}$ and $DyBa_{1.7}Sr_{0.3}Cu_3O_{7-\delta}$ may be due to the influence of the elastic anomaly existing at a higher temperature. Interestingly, for $DyBa_2Cu_3O_{7-\delta}$, the deviation starts at a slightly lower temperature of 140 K for the shear mode compared to the longitudinal mode where the deviation starts at 200 K. On the other hand for $DyBa_{1.4}Sr_{0.6}Cu_3O_{7-\delta}$ where the step-like anomaly is strongly suppressed, the ultrasonic shear and longitudinal velocities generally obey the calculated anharmonicity curve.

The step-like anomaly observed in $DyBa_2Cu_3O_{7-\delta}$ is probably oxygen content related as observed in previous reports for other

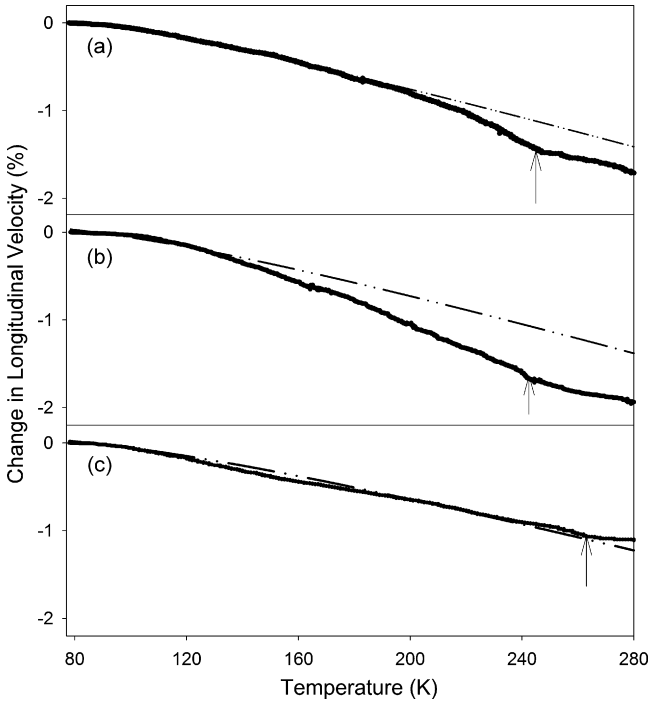

Fig. 4. Fits of Eq. (2) (thin broken lines) to the temperature dependencies of the longitudinal wave for $DyBa_{2-x}Sr_xCu_3O_{7-\delta}$ (a) $x = 0$; (b) $x = 0.3$; and (c) $x = 0.6$. The expressions were fitted to the data using the values of Debye temperatures in Table 3. The arrow points to the location of the step-like anomaly.

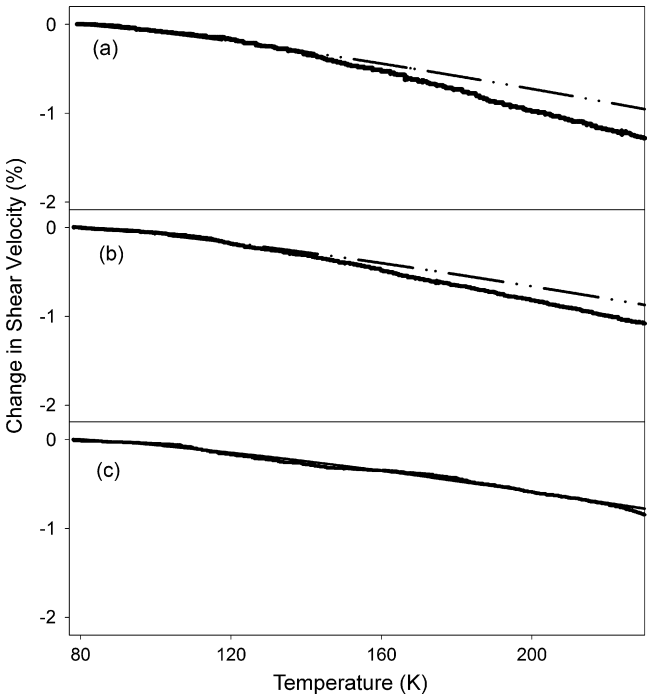

Fig. 5. Fits of Eq. (2) (thin broken lines) to the temperature dependencies of the shear wave velocities for $DyBa_{2-x}Sr_xCu_3O_{7-\delta}$. (a) $x = 0$; (b) $x = 0.3$; and (c) $x = 0.6$. The expressions were fitted to the data using the values of Debye temperatures in Table 3.

RE123 materials. Ultrasonic velocity measurements in oxygenated and oxygen depleted RE123 samples consistently demonstrated that step-like anomalies above 200 K disappeared after oxygen reduction confirming the oxygen related character of the anomaly [16,17,28,42]. Nevertheless, previous ultrasonic report on differently annealed Gd1113 samples which is isostructural to RE123, indicates that oxygen content is not the key factor influencing the anomaly [43]. Instead, the anomaly has been suggested to be due to a phase transition involving different orthorhombic superstructures which forms as a result of oxygen ordering in Cu–O chains of RE123 materials [1,17,28]. An attenuation peak around the same temperature range was often reported to accompany the step-like anomaly [16,44] and is believed to be caused by mobile oxygen atoms involved in the phase transition.

Our results for $DyBa_{2-x}Sr_xCu_3O_{7-\delta}$ ($x = 0$–0.6) in this study which showed step-like anomalies for all samples indicate existence of oxygen ordering in all the samples. However, the fact that the step-like anomalies were softened by the Sr substitutions indicates some degree of weakening of the oxygen ordering process. The Sr substitution which caused changes in cell volume and bonding lengths between constituent atoms may have affected the extent of oxygen rearrangement taking place in Cu–O chains. It is also possible that the reduction in the slope change of the step-like anomaly may be caused by other factors such as differences in microstructure or oxygen content of the samples. However, differences in microstructure of the samples are not likely to influence the step-like anomaly as the microstructures of the $x = 0.3$ and $x = 0.6$ samples are quite similar although their step-like anomalies showed large differences in slope change. On the other hand, a discussion on the possibility of small differences in oxygen content influencing the anomaly is very intricate. Previous studies on Sr substitution at Ba-sites of Nd123 and Pr123 reported only small variation in oxygen content as the result of the substitution [25,35]. As such, a large difference in oxygen contents of $DyBa_{2-x}Sr_xCu_3O_{7-\delta}$ samples is not expected. Instead, the reduction in the slope change of the step-like anomalies can be attributed to reduction in the degree of oxygen ordering. In addition, quite recently, elemental substitution in RE123 was reported to introduce some disparity in weight of insulating planes which in turn was suggested to cause the non-linear drop in $T_{c\ zero}$ [27]. Additionally, our results, which showed a non-linear drop of T_c with Sr substitution is also accompanied by a non-linear reduction of the slope change of the step-like anomalies. Nevertheless, whether the step-like anomalies or the degree of oxygen ordering have a direct influence on T_c is not known.

On the other hand, the reduction in electron–phonon coupling constant (λ) with Sr may be due to changes in internal chemical pressure of the 123 unit cell due to substitution of the smaller Sr^{2+} in place of Ba^{2+} [45]. Although the role of the Ba-site of RE123 in superconductivity is not clear [46] the present work has shown that substitution of non-magnetic Sr^{2+} at the site affects the strength of electron–phonon interaction and is detrimental for Cooper pair formation in CuO planes.

4. Conclusion

Ultrasonic longitudinal and shear velocity measurements have been performed in Ba-site substituted $DyBa_{2-x}Sr_xCu_3O_{7-\delta}$ ($x = 0$, 0.3, 0.6) ceramic superconductors. Step-like anomalies were observed above 200 K and were suggested to be due to oxygen ordering in CuO chains. Sr substitution caused a gradual but non-linear reduction in the slope change of the step-like anomalies which indicates a reduction in the degree of oxygen ordering due to the substitution. The decrease in electron–phonon coupling constant, λ with Sr substitution is may be due to changes in internal pressure of the unit cell that affected electron–phonon coupling in the system.

Acknowledgement

Authors would like to thank the Academy of Sciences Malaysia for supporting this research under the Scientific Advancement Fund Allocation (SAGA), Grant No. P16.

References

[1] J.G. Bednordz, K.A. Muller, Z. Phys. B – Condens. Matter B64 (1986) 189–193.
[2] M.K. Wu, J.R. Ashburn, C.J. Torng, P.H. Hor, R.L. Meng, L. Gao, Z.J. Huang, Y.Q. Wang, C.W. Chu, Phys. Rev. Lett. 58 (1987) 908–910.
[3] Z.Z. Sheng, A.M. Hermann, Nature 332 (1988) 55–58.
[4] H. Maeda, Y. Tanaka, M. Fukutomi, T. Asano, Japan. J. Appl. Phys. 27 (1988) 209–210.
[5] S.N. Putilin, E.V. Antipov, O. Chmaissem, M. Marezio, Nature 362 (1993) 226–228.
[6] Lanzara, P.V. Bogdanov, X.J. Zhou, S.A. Kellar, D.L. Feng, E.D. Lu, T. Yoshida, H. Eisaki, A. Fujimori, K. Kishio, J.I. Shimoyama, T. Nodall, S. Uchida, Z. Hussain, Z.-X. Shen, Nature 412 (2001) 510–514.
[7] Jinho Lee, K. Fujita, K. McElroy, J.A. Slezak, M. Wang, Y. Aiura, H. Bando, M. Ishikado, T. Masui, J.X. Zhu, A.V. Balatsky, H. Eisaki, S. Uchida, J.C. Davis, Nature 442 (2006) 546–550.
[8] Y.B. Saddeek, J. Alloys Compd. 467 (2009) 14–21.
[9] G. Murali Krishna, N. Veeraiah, N. Venkatramaiah, R. Venkatesan, J. Alloys Compd. 450 (2008) 477–485.
[10] M.V.S. Reddy, M.S. Reddy, C.N. Reddy, R.P.S. Chakradhar, J. Alloys Compd. (2008), doi:10.1016/j.jallcom.2008.12.102.
[11] Y.B. Saddeek, E.R. Shaaban, Kamal. A. Aly, I.M. Sayed, J. Alloys Compd. (2008), doi:10.1016/j.jallcom.2008.11.063.
[12] G.A. Lalitha, D. Dasb, D. Bahadur b, P. Venugopal Reddy, J. Alloys Compd. 464 (2008) 6–8.
[13] R.I. Zainullina, N.G. Bebenin, V.V. Ustinov, Ya.M. Mukovskii, J. Alloys Compd. 467 (2009) 22–26.
[14] K. Hui, Z. Changfei, J. Alloys Compd. (2008), doi:10.1016/j.jallcom.2008.12.030.
[15] J. Yi, H. Kong, C. Zhu, J. Alloys Compd. (2008), doi:10.1016/j.jallcom.2008.06.132.
[16] D.P. Almond, Q. Wang, J. Freestone, E.F. Lambson, B. Chapman, G.A. Saunders, J. Phys.: Condens. Matter 1 (1989) 6853–6864.
[17] A.K. Yahya, R. Abd Shukor, Supercond. Sci. Technol. 11 (1998) 173–178.
[18] T. Fukami, A.A. Youssef, Y. Horie, S. Mase, Physica C 161 (1989) 34.
[19] M. Cankurtaran, G.A. Saunders, Q. Wang, H. Celik, Supercond. Sci. Technol. 8 (1995) 811–815.
[20] N.A.N. Jaafar, R. Abd-Shukor, Phys. Lett. A 288 (2001) 105–110.
[21] C. Fanggao, M. Cankurtaran, G.A. Saunders, D.P. Almond, P.J. Ford, A. Al-Kheffaji, Supercond. Sci. Technol. 3 (1990) 546–555.
[22] S. Satyavathi, M. Muralidhar, V. Hari Babu, R. Ravinder Reddy, P. Venugopal Reddy, J. Alloys Compd. 209 (1994) 329–335.
[23] A.K. Yahya, R. Abd Shukor, Physica C 314 (1999) 117–124.
[24] Y. Shimakawa, Physica C 202 (1992) 199.
[25] T. Wuernisha, Y. Takahashi, K. Takase, Y. Takano, K. Sekizawa, J. Alloys Compd. 377 (2004) 216–220.
[26] F. Licci, A. Gauzzi, M. Marezio, G.P. Radaelli, R. Masini, C. Chaillout-Bougerol, Phys. Rev. B 58 (1998) 15208–15217.
[27] E.W. Barrera, M.P. Rojas Sarmiento, L.F. Rincon, D.A. Landínez Tellez, J. Roa-Rojas, Phys. Status Solidi (c) Conf. 4 (2007) 4306–4310.
[28] A.K. Yahya, N.A. Hamid, R. Abd-Shukor, H. Imad, Ceram. Int. 30 (2004) 1597–1601.
[29] R. Abd Shukor, Solid State Commun. 142 (2007) 587–590.
[30] R. Abd-Shukor, C.T. Vui, Physica B 357 (2005) 253–258.
[31] S.C. Lakkad, J. Appl. Phys. 42 (1971) 4277–4281.
[32] B. Buchner, U. Callieb, H.D. Jostarndt, W. Schlabitz, D. Wohlleben, Solid State Commun. 73 (1990) 357–361.
[33] K. Donnelley, J.M.D. Coey, S. Tomlinson, J.M. Greneche, Physica C 156 (1988) 579.
[34] T. Krekels, H. Zou, Tendeloo, G. Van, D. Wagener, M. Buchgeister, S.M. Hosseini, P. Herzog, Physica C 196 (1992) 363–368.
[35] G.B. Song, J.K. Liang, L.T. Yang, Q.L. Liu, G.Y. Liu, H.F. Yang, G.H. Rao, J. Alloys Compd. 370 (2004) 302–306.
[36] J.B. Wachtman, W.E. Tefft, D.G. Lam, C.S. Apstein, Phys. Rev. 122 (1961) 1961.
[37] Y.P. Varshni, Phys. Rev. B 2 (1970) 3952–3958.
[38] S.P. Dodd, M. Cankurtaran, B. James, J. Mater. Sci. 38 (2003) 1107–1115.
[39] R. Ravinder Reddy, P. Venugopal Reddy, Physica C 265 (1996) 96–106.
[40] M. Levy, M. Xu, B.K. Sarma, K.J. sun, Physical Acoustics (XX) Ultrasonics of High-T_c and other Unconventional Superconductors, Academics Press, New York, 1992, p. 295.
[41] L. Sihan, H. Yusheng, W. Chongde, S. Zhaohui, Supercond. Sci. Technol. 2 (1989) 145–148.
[42] Q. Wang, G.A. Saunders, D.P. Almond, M. Cankurtaran, K.C. Goretta, Phys. Rev. B 52 (1995) 3711–3725.
[43] A.K. Yahya, A.K. Koh, R. Abd Shukor, Phys. Lett. A 259 (1999) 295–301.
[44] A.K. Yahya, A. Ishak, I. Hamadned, R. Abd-Shukor, Mater. Sci. Forum 517 (2006) 17–20.
[45] V.N. Vieira, P. Pureur, J. Schaf, Physica C 353 (2001) 241–250.
[46] X.N. Ying, Y.N. Wang, Solid State Commun. 139 (2006) 493–496.